

RESEARCH

Open Access



Cardiac substructure dose distributions in node-positive and node-negative breast cancer patients undergoing 3D-CRT: comparing the predictive accuracy of mean heart dose and mean left ventricular dose

Mohammad Gunda Nuruddeen^{1,2}, Noor Khairiah A Karim^{1,3,4*} , Gokula Kumar A/L Appalanaido¹, Mohd Hafiz Mohd Zin^{1,3}, Khairil Amir Sayuti⁵ and Mohamad Nazrulhisham Mad Naser⁶

Abstract

Background and purpose Cardiotoxicity is a concern, especially in left breast cancer (BC) radiotherapy (RT), and accurate dosimetry is essential for minimizing cardiac exposure. This study evaluated the radiation exposure of cardiac substructures in node-positive and node-negative BC patients who underwent three-dimensional conformal therapy (3D-CRT) and compared the predictive accuracy of mean heart dose (MHD) and mean left ventricular dose (MLVD) in estimating dose distribution to cardiac substructures.

Materials and methods This study included 55 patients with left-sided breast cancer, comprising 39 with node-positive and 16 with node-negative disease. All underwent adjuvant whole-breast irradiation using 3D-CRT. The heart, ventricles, atria, right coronary (RC), left anterior descending coronary (LADCA), and left circumflex (LCx) arteries were contoured. Dosimetric distributions were evaluated, and Pearson's correlation and linear regression analyses were used to assess the relationship between cardiac substructures.

Results The distribution of doses to cardiac substructures was heterogeneous, with LADCA receiving the highest doses: 15.6 Gy in node-positive and 13.2 Gy in node-negative breast cancer patients. Linear regression analysis revealed a weak to moderate predictive ability of MHD/MLVD to predict doses received by the cardiac substructure in both groups, with MLVD demonstrating marginally better results. For node-positive patients, the analysis revealed an R^2 of 0.40 ($p < 0.001$) for the association between MHD and LADCA and an R^2 of 0.45 ($p < 0.001$) for MLVD and LADCA. In node-negative patients, the R^2 values were 0.27 ($p < 0.001$) for MHD versus LADCA and 0.30 ($p < 0.03$) for MLVD versus LADCA. Pearson's correlation analysis for node-positive patients indicated $r = 0.63$ ($p < 0.001$) for MHD versus LADCA and $r = 0.67$ ($p < 0.001$) for MLVD versus LADCA. For node-negative patients, the correlation coefficients were $r = 0.52$ ($p < 0.001$) for MHD versus LADCA and $r = 0.54$ ($p < 0.001$) for MLVD versus LADCA.

*Correspondence:
Noor Khairiah A Karim
drkhairiah@usm.my

Full list of author information is available at the end of the article



© The Author(s) 2025. **Open Access** This article is licensed under a Creative Commons Attribution-NonCommercial-NoDerivatives 4.0 International License, which permits any non-commercial use, sharing, distribution and reproduction in any medium or format, as long as you give appropriate credit to the original author(s) and the source, provide a link to the Creative Commons licence, and indicate if you modified the licensed material. You do not have permission under this licence to share adapted material derived from this article or parts of it. The images or other third party material in this article are included in the article's Creative Commons licence, unless indicated otherwise in a credit line to the material. If material is not included in the article's Creative Commons licence and your intended use is not permitted by statutory regulation or exceeds the permitted use, you will need to obtain permission directly from the copyright holder. To view a copy of this licence, visit <http://creativecommons.org/licenses/by-nc-nd/4.0/>.

Conclusion Radiation exposure to cardiac substructures during 3D-CRT for left breast cancer was heterogeneous, with the LADCA receiving the highest mean dose, followed by the LV. MLVD demonstrated superior predictive accuracy over mean heart dose (MHD) for estimating doses to critical substructures, particularly in node-positive patients.

Keywords Left breast cancer, 3D-CRT, Mean heart dose, Mean left ventricular dose, Cardiac substructures

Introduction

Breast cancer (BC) is the most prevalent malignancy among women worldwide, with radiotherapy (RT) playing a pivotal role as an adjuvant therapy to improve local control and overall survival outcomes following breast-conserving surgery or mastectomy [1–4]. BC RT is among the most widespread therapies in radiation oncology [5]. It could be based on more sophisticated methods, such as intensity-modulated radiation therapy (IMRT) and volumetric-modulated arc therapy (VMAT), or on traditional three-dimensional conformal radiotherapy (3D-CRT) [6]. The more advanced and technology-driven RT techniques have reduced acute and late toxicities and improved cosmetic outcomes. However, they are only available in some centres and have inherent shortcomings [5].

Although various studies have shown that the use of modern RT techniques has reduced cardiac exposure during RT of the left breast, epidemiological data show an increased risk of cardiovascular complications even after exposure to lower doses [3, 7–9]. Exposure to low doses does not mean absolute safety because there is no threshold dose limit below which the best curative outcomes are accomplished with the least or zero tendency toward cardiotoxicity [8, 10, 11].

Node-positive BC patients undergoing RT present additional complexity because a larger RT field is needed to accommodate affected lymph nodes. This results in a larger heart volume being irradiated, which can increase the dose received by cardiac substructures, potentially leading to cardiotoxicity [12].

The heart is typically considered a singular organ-at-risk (OAR) during RT planning, with the mean heart dose (MHD) frequently utilized to quantify the exposures received by the heart and its substructures [10, 13, 14]. However, MHD has limitations in capturing the detailed radiation exposure of critical cardiac substructures, such as the left anterior descending coronary artery (LADCA), left ventricle (LV), and left atrium (LA), which are more proximally located to the treatment fields [2, 9, 14–21]. This limitation is particularly significant in left-sided BC patients, where the heart's anterior and apical regions of the heart receive relatively higher doses. Recent studies have highlighted the shortcomings of MHD as a surrogate for substructure-specific doses, demonstrating that it is not a reliable indicator of the dose received by cardiac substructures [14, 19, 22].

While delineating these substructures as distinct organs-at-risk (OARs) is essential for precision heart-sparing therapy, practical challenges including time constraints, non-contrast CT visibility, and clinical workflow demands often limit routine implementation.

Therefore, there is a need for a detailed radiation dose distribution received by the cardiac substructures, and doing so requires contouring of each critical substructure. The heart is an intricate organ with many vital substructures, and the gold standard for cardiac and substructure delineation is manual segmentation following international contouring guidelines [13, 23]. Moreover, delineating the heart and its substructures is not a routine part of the RT planning procedure, considering the number and intricacy of the structures concerned. It is also tedious and time-intensive, especially when the patient throughput is high [13, 23, 24]. For example, the critical OARs during left breast 3D-CRT, the coronary arteries, may not be entirely visible because of their tortuous nature and the non-contrast, thick-slice CT simulation images used in delineation [7, 9, 10, 25–27].

The LV is the largest and most muscular cardiac chamber, making it the easiest cardiac substructure to delineate. Regarding proximity to the treatment field during 3D-CRT of the left breast, the LV is the closest cardiac substructure [28, 29]. The LADCA (a radiosensitive substructure and a typical site frequently implicated in ischemic heart disease) is located within the interventricular groove [13, 30]. According to one study, radiation exposure to a volume of the LV receiving 5 Gy predicted significant coronary events compared with MHD [31].

These findings regarding the LV and its ease of delineation highlight the necessity of using it as a predictor of doses received by cardiac substructures, possibly even surpassing the MHD.

This study aimed to evaluate the radiation exposure of cardiac substructures in node-positive and node-negative BC patients who underwent 3D-CRT and compare the predictive accuracy of MHD and MLVD in estimating the dose distribution to cardiac substructures.

Materials and methods

Study population

This retrospective study included 55 adult female patients diagnosed with left BC, comprising thirty-nine node-positive and sixteen node-negative patients. All patients received adjuvant radiotherapy using 3D-CRT,

with whole-breast irradiation for those who underwent breast-conserving surgery and chest wall (CW) irradiation for post-mastectomy patients. This was performed using an Elekta TM 160 Agility Leaf Linear Accelerator at AMDI, Universiti Sains Malaysia, between January and December 2017. Patients treated for other malignancies, who received a different RT technique, or who had unavailable computed tomography (CT)-based RT planning data in the archive during the study period were excluded. The university's ethics committee approved the study (USM/JEPeM/16110523).

CT simulation

Each patient underwent a 3 mm slice computerized axial tomography simulation scan while the Deep breathing technique was employed. The patients were positioned supine on a tilted simulation table (with a breast board) with their arms raised above the head. The inferior border of the scan field was centered 1.5 cm inferior to the right sub-mammary crease, whereas the superior border was centered at the sternum and 2nd rib joint. No contrast agents were administered. The acquired CT data were imported in DICOM format into the Monaco 5.1 treatment planning system (TPS) (Elekta Medical System, Crawley, UK).

Target volume and organs at risk (OAR) delineation

At Monaco 5.1 TPS (Elekta Medical System, Crawley, UK), the skin is semi-automatically delineated the skin by the software. The target volume (TV) was defined using the Radiation Therapy Oncology Group Breast Contouring Atlas (RTOG), which adheres to consensus standards

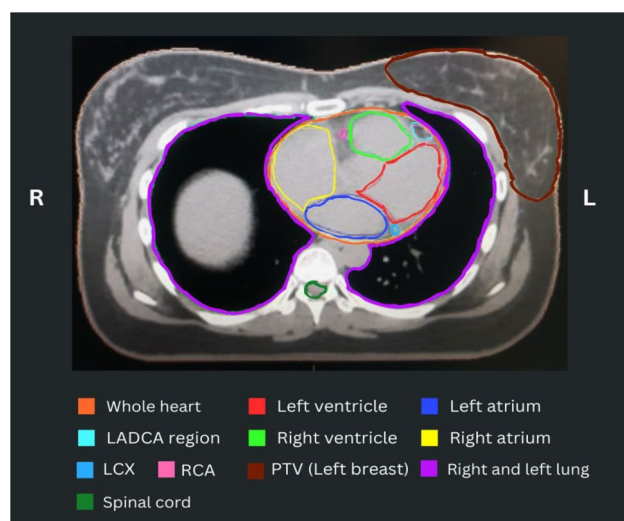


Fig. 1 Axial CT simulation image of the manual cardiac substructures and other OAR delineation (coloured lines are drawn around the whole heart, substructures, and lungs). PTV=planning target volume, LADCA=left anterior descending coronary artery, LCX=left circumflex artery, and RCA=right coronary artery)

for defining anatomical borders and clinical CWs. For OAR, the contours of the complete heart include the ventricle's infundibulum, right auricle, apex, and all visible myocardia. The spinal cord and left lung were among the contoured OARs. To achieve the objective of this study, each patient's cardiac chambers (LA, LV, RA, and RV), LADCA, left circumflex artery (LCx), and right coronary artery (RCA) were contoured on the Monaco 5.1 TPS workstation (Fig. 1). Contouring was achieved after dedicated cardiac substructure segment identification and contouring training by an experienced cardiac radiologist and oncologist. The atlas for cardiac delineation published by Duane et al., [7], served as a valuable reference. A cardiac radiologist reviewed all contours and made any necessary amendments before approving the generation of dose-volume histograms (DVHs).

Treatment planning

Conventional 3D-CRT tangential photon fields conforming to the delineated treatment volume per the RTOG atlas were employed. The tangential field borders extend caudally (1.5 cm), less than 2 cm cranially from the humeral head, medially at the Centre, and laterally at the anterior edge of the serratus anterior. Most patients were treated with 10 or 6 megavolt photons at a dose of 42.56 Gy (range: 41.8–43.2 Gy). The dose was prescribed to the mid-plane at two-thirds the distance along a tangential line extending from the midpoint of the half-beam blocked tangential fields to the skin surface. Treatment comprised 16 daily fractions delivered over 3.5 weeks, with five fractions administered weekly. The dose was initially prescribed to the mid-plane at a two-thirds distance from a tangential line that links the midpoint of $1/2$ -beam-blocked tangents to the skin. The plan was subsequently optimized using beam angles, collimator angles, and wedges. The dose limits to the heart were, per RTOG references, as follows: <5% of the cardiac volume should receive 40 Gy and less than 10% of the cardiac volume should receive 25 Gy.

Patient characteristics, clinical information, CT-based radiation therapy planning data, and follow-up information were retrospectively collected from patient histories. Dose distributions were calculated, and DVHs were generated for all the contoured structures. The equivalent dose in fractions of 2 Gy (EQD2) was calculated using the linear quadratic model with a cardiac alpha/beta ratio 2.5 to evaluate the cardiac dosimetric parameters [19, 32].

Statistical analysis

A descriptive statistical analysis of the radiation doses was conducted, presenting the values of the mean, standard deviation, and range. Mean dose differences between node-positive and node-negative groups for the heart and cardiac substructures were analysed using

independent (unpaired) t-tests. Pearson's correlation analysis was performed to determine the associations between MHD, and the doses received by the contoured cardiac substructures. Similarly, the research investigated the relationship between the MLVD, and the doses received by contoured heart substructures. Linear regression analysis was employed to evaluate the predictive accuracy of MHD and MLVD in estimating the dose to each substructure. One-sample t-test was used to compare MHD and MLVD against the mean doses received by individual cardiac substructures. Statistical significance was set at $p < 0.05$. All statistical analyses were conducted using JASP software (Version 0.18.1) [33].

Results

Retrospective dosimetric analysis was available for 55 female left-BC patients who underwent 3D-conformal hypo-fractionated RT using 6 or 10 MV photons. The mean age of the patient cohort was 50 years (range: 24–80

years). Most of the BC patients were diagnosed with invasive ductal carcinoma (IVC) and underwent mastectomy. The radiation dose prescribed for the patients was 42.56 Gy in 16 fractions. Table 1 summarizes the patients' baseline demographics and their tumour and treatment characteristics.

The dose constraints to the heart were met for all patients ($V25Gy < 10\%$, $V40Gy < 5\%$). Significant interpatient dose variability was observed across the contoured cardiac substructures. The MHD for the entire cohort was 3.4 ± 0.9 Gy, ranging from 2.0 Gy to 6.3 Gy. The mean MHD in node-positive patients was marginally higher than that in node-negative patients (3.5 ± 0.9 Gy vs. 3.2 ± 0.9 Gy, $p = 0.12$).

The LADCA received the highest dose among the cardiac substructures, with a mean value of 15 ± 6.6 Gy (range: 10.6–21.8 Gy) for the entire cohort. Patients with node-positive BC received a mean LADCA dose of 16.7 ± 6.4 Gy (range: 10.6–21.8 Gy), whereas node-negative patients received a mean LADCA dose of 14.2 ± 5.9 Gy (range: 12.6–21.2 Gy), all of which significantly exceeded the MHD.

It is followed by LV with a mean dose of dose of 4.5 ± 2.3 Gy (range: 3.3–9.8 Gy) across all participants. Node-positive patients had an MLVD of 5.8 ± 3.1 Gy (range: 3.3–9.8 Gy), whereas node-negative patients had an MLVD of 3.2 ± 1.2 Gy (range: 3.4–6.3 Gy).

In contrast, the right atrium (RA) received the lowest radiation exposure, with a mean dose of 0.7 ± 0.2 Gy (range: 0.3–1.5 Gy) for node-positive patients and 0.6 ± 0.1 Gy (range: 0.4–0.9 Gy) for node-negative patients.

LCx received the lowest dose among the contoured coronary arteries, with a mean value of 0.9 ± 1.1 Gy (range: 2.0–5.3 Gy) for the entire cohort. Node-positive patients received a mean LCx dose of 1.1 ± 1.1 Gy (range: 2.0–5.3 Gy), whereas node-negative patients received a mean LCx dose of 0.8 ± 0.2 Gy (range: 2.0–5.3 Gy). (Figures 2 and 3).

One sample t-test revealed significant differences between MHD and the mean doses administered to the delineated cardiac substructures, as well as between MLVD and the mean doses received by the contoured cardiac substructures in both node-positive and node-negative breast cancer patients ($p < 0.05$).

Pearson's correlation analysis revealed a range of correlations involving MHD and cardiac substructure doses, as well as MLVD and cardiac substructure doses. Notably, a moderate positive correlation was identified between MHD and RV in node-positive BC patients ($r = 0.69$, $p < 0.001$), while a strong correlation was found in node-negative patients ($r = 0.73$, $p < 0.001$). Strong positive correlations were found between MLVD and RV in node-positive patients ($r = 0.90$, $p < 0.001$) and node-negative

Table 1 Patients' baseline demographics and tumour characteristics

| Characteristic | n(range)/ (%) |
|---------------------------------|-----------------------|
| Total Patients | 55 (100%) |
| Age in years | 50 (24–80) |
| Type of cancer | |
| Invasive ductal carcinoma | 49 (89.1%) |
| Ductal carcinoma in situ | 2 (3.6%) |
| Invasive lobular carcinoma | 2 (3.6%) |
| Lobular carcinoma in situ | 2 (3.6%) |
| Tumor classification | |
| T1 | 11 (20%) |
| T2 | 34 (61.8%) |
| T3 | 8 (14.5%) |
| T4 | 2 (3.6%) |
| Nodal status | |
| N0 | 16 (29.1%) |
| N1 | 17 (30.9%) |
| N2 | 18 (32.7%) |
| N3 | 4 (7.3%) |
| Metastasis Status | |
| M0 | 42 (76.4%) |
| M1 | 8 (14.5%) |
| Mx | 5 (9.1%) |
| Surgery type | |
| Mastectomy (without prosthesis) | 43 (78%) |
| Mastectomy (with prosthesis) | 0 (0%) |
| Breast conservation surgery | 12 (22%) |
| Prescribed dose | 42.56 Gy/16 fractions |
| Adjuvant therapy | |
| Chemotherapy | 33 (60%) |
| Endocrine therapy | 17 (30.9%) |
| Targeted therapy | 5 (9.1%) |
| - Herceptin | 4 (7.3%) |
| - Pembrolizumab | 1 (1.8%) |

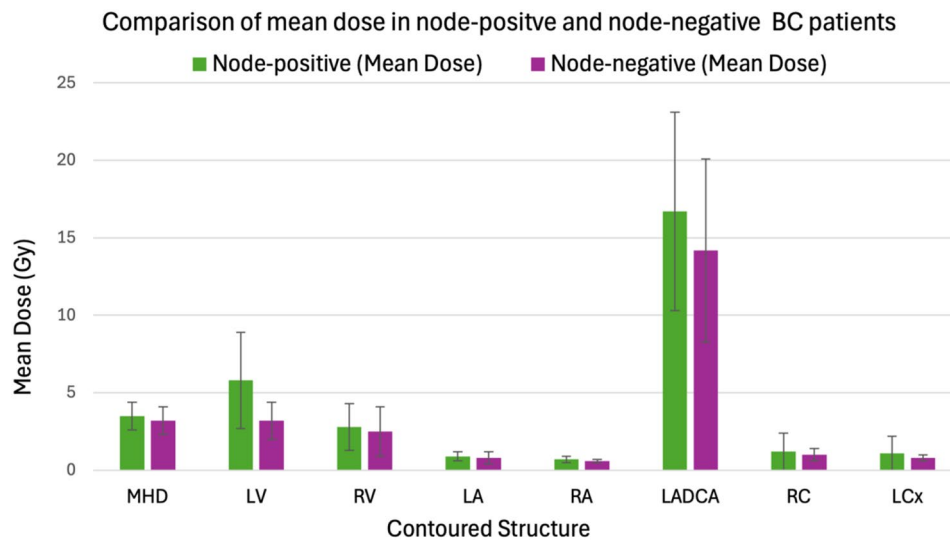


Fig. 2 Mean values of the dose received by the heart and contoured substructures in node-positive and node-negative BC patients. (BC = breast cancer, MHD = mean heart dose, LV = left ventricle, RV = right ventricle, LA = left atrium, RA = right atrium, RC = right coronary artery, LADCA = left anterior coronary descending artery, LCx = left circumflex artery)

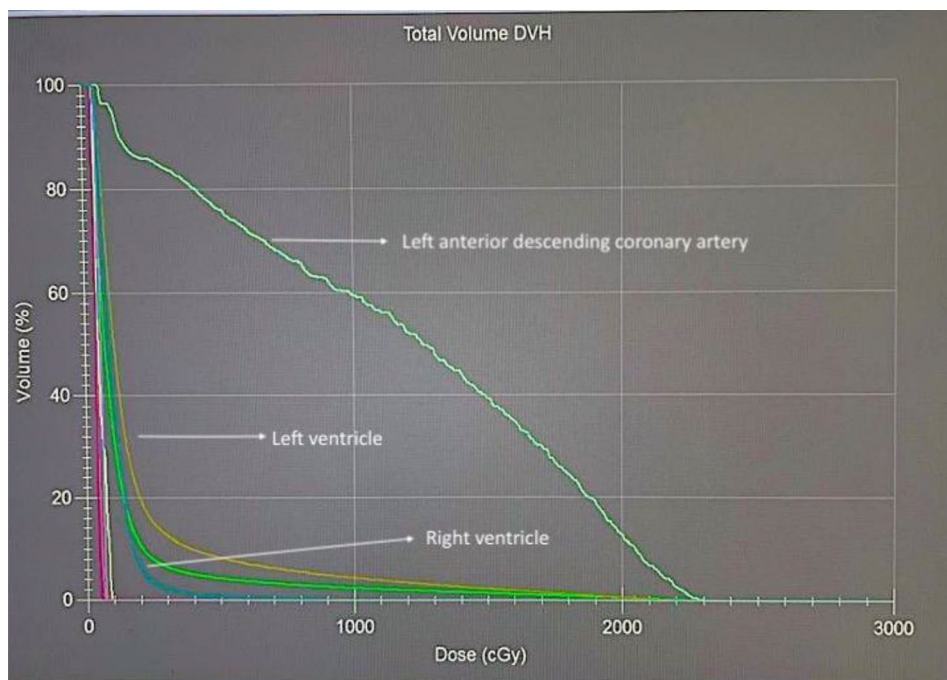


Fig. 3 DVH of the contoured cardiac substructures for a single patient. The arrows point to the dose volume curves of the LADCA and LV

patients ($r=0.76$, $p<0.001$). Moderate positive correlations were noted between MHD and mean LADCA doses in these groups (node-positive: $r=0.63$, $p<0.001$; node-negative: $r=0.52$, $p=0.039$). There were also moderate correlations between MLVD and LADCA doses, with $r=0.67$ ($p<0.01$) in node-positive patients and $r=0.53$ ($p<0.031$) in node-negative patients. In contrast, weak positive correlations were observed between MHD and mean RA doses, with $r=0.17$ ($p=0.51$) in

node-positive patients and $r=0.23$ ($p=0.36$) in node-negative BC patients. A negative correlation was noted between MLVD and LA in node-negative patients with $r=-0.03$ ($p=0.9$) (Figs. 4 and 5).

The linear regression analysis of MHD and the mean LADCA dose revealed moderate correlations for node-positive BC patients ($R^2 = 0.40$, $p<0.001$) and weak correlations for node-negative patients ($R^2 = 0.27$, $p<0.01$). Similarly, the analysis between MLVD and the mean

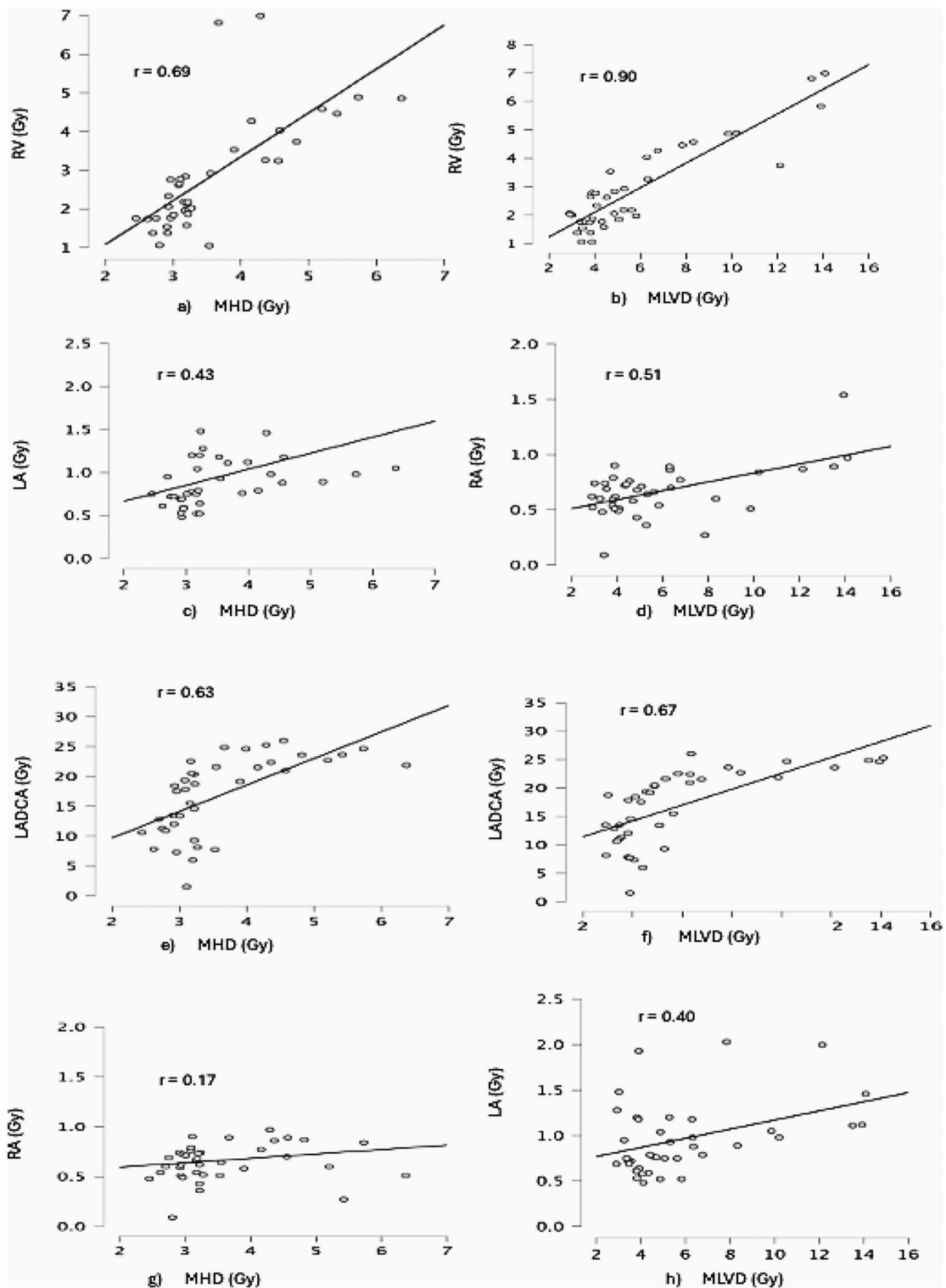


Fig. 4 Scatter plots (a-h) showing the relationship between MHD and MLVD vs. dose to cardiac substructures in Gy for node-positive BC patients. (MHD=mean heart dose, MLVD=mean left ventricular dose, RV=right ventricle, LV=left ventricle, RA=right atrium, LA=left atrium, LADCA=left anterior descending coronary artery)

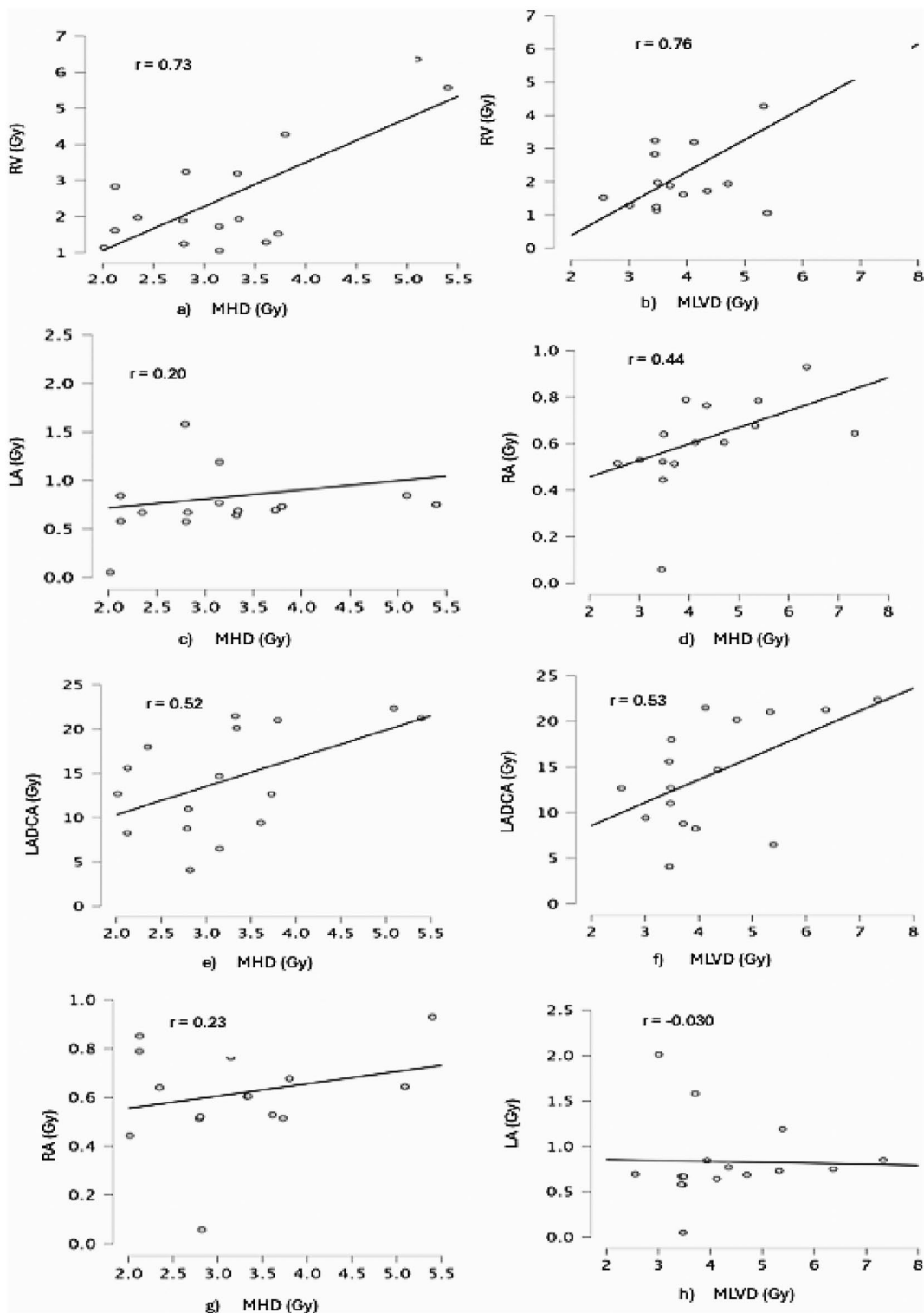


Fig. 5 Scatter plots (a-h) showing the relationship between MHD and MLVD vs. dose to cardiac substructures in Gy for node-negative BC patients. (MHD= mean heart dose, MLVD= mean left ventricular dose, RV= right ventricle, LV=left ventricle, RA= right atrium, LA=left atrium, LADCA= left anterior descending coronary artery)

Table 2 Linear regression coefficient values between MHD and MLVD versus the cardiac substructures for node-positive and node negative BC patients

| Independent variable | Dependent variable | Coefficient of determination | | | |
|----------------------|--------------------|------------------------------|---------|---------------------------|---------|
| | | Node-positive BC patients | | Node-negative BC patients | |
| | | R ² | P value | R ² | P value |
| MHD | MRV | 0.489 | <0.001 | 0.54 | 0.007 |
| MHD | MLA | 0.15 | 0.005 | 0.04 | <0.001 |
| MHD | MRA | 0.031 | <0.283 | 0.05 | 0.374 |
| MHD | MLADCA | 0.40 | <0.001 | 0.27 | <0.001 |
| MHD | MRC | 0.096 | 0.055 | 0.42 | <0.001 |
| MHD | MLCX | 0.10 | 0.061 | 0.12 | 0.037 |
| MLVD | MRV | 0.60 | <0.001 | 0.58 | <0.001 |
| MLVD | MLA | 0.16 | 0.012 | 0.01 | 0.013 |
| MLVD | MRA | 0.29 | <0.001 | 0.20 | 0.005 |
| MLVD | MLADCA | 0.45 | <0.001 | 0.30 | <0.03 |
| MLVD | MRC | 0.22 | 0.002 | 0.54 | 0.007 |
| MLVD | MLCX | 0.10 | 0.131 | 0.04 | <0.001 |

(MHD=mean heart dose, MLVD=mean left ventricular dose, MRV=mean right ventricle, MRA=mean right atrium, MLA=mean left atrium, MLADCA=mean left anterior descending coronary artery, MLCx=mean left circumflex artery, MRC=mean right coronary artery)

LADCA dose indicated moderate correlations in both node-positive BC patients ($R^2 = 0.45$, $p < 0.001$) and node-negative BC patients ($R^2 = 0.30$, $p < 0.03$) BC patients.

For various cardiac substructures, the regression analysis examining the relationship between MHD and the mean doses received by the RV, LA, and LCx arteries showed R^2 values of ($R^2 = 0.48$, $p < 0.001$), ($R^2 = 0.15$, $p < 0.005$), and ($R^2 = 0.10$, $p = 0.06$) for node-positive patients, and ($R^2 = 0.54$, $p < 0.001$), ($R^2 = 0.04$, $p < 0.001$), and ($R^2 = 0.12$, $p = 0.037$) for node-negative patients. In the same vein, the regression analysis between MLVD and the mean doses received by the RV, LA, and LCx arteries revealed R^2 values of ($R^2 = 0.60$, $p < 0.001$), ($R^2 = 0.16$, $p = 0.012$), and ($R^2 = 0.10$, $p = 0.131$) for node-positive patients, whereas for node-negative patients, the R^2 were ($R^2 = 0.58$, $p < 0.001$), ($R^2 = 0.01$, $p = 0.013$), and ($R^2 = 0.04$, $p < 0.001$) respectively (Table 2).

These results indicate that the doses received by the LADCA and various important cardiac structures can be inferred from MLVD, with MLVD showing greater accuracy in predicting the doses received by LADCA and these critical cardiac substructures than MHD.

Discussion

Adjuvant RT, along with surgery, chemotherapy, and hormonal therapy, is crucial for BC therapy; however, it increases the risk of radiation-induced cardiotoxicity [2, 3, 25]. Modern RT techniques have decreased cardiac radiation exposure; however, the risk of RT-induced cardiotoxicity remains [3, 10]. The risk increases with increasing cardiac radiation exposure, with

intra-individual heterogeneity of cardiac dose-volume parameters being a concern [10, 14, 34, 35]. MHD is a commonly used surrogate for assessing potential cardiotoxic effects after BC RT. It is influenced by factors affecting its predictive efficacy in cardiac substructure doses [3, 10, 35]. Studies suggest that doses to individual cardiac substructures should be considered separately during RT rather than using MHD as a proxy for all cardiac substructures [2, 22, 35]. This study assessed the accuracy of the MLVD in predicting the doses received by cardiac substructures. Our results show that the predictive accuracy of the MLVD is greater than that of the commonly used MHD in predicting the doses received by the cardiac substructures, as evidenced in Table 2.

Radiation dose distribution to the cardiac substructures was heterogeneous with the LADCA receiving the highest amount of radiation followed by the LV, which received a much higher dose than some of the cardiac substructures. These research outcomes align with those reported by Van Den Bogaard et al. [31] and Costin et al. [36]. Similarly, Prunarety et al. [37] demonstrated in their study that the dose distribution to the heart and its substructures varied significantly. Additionally, a study by Nilsson et al. [38], assessed the distribution of coronary artery stenosis among BC patients to determine the correlation between the doses received during RT and the location of stenosis. They discovered that LV and LADCA received the highest doses, with the middle and lower segments of LADCA receiving even higher doses than the upper segment.

The high doses received by LADCA and LV correspond to their anatomical closeness to the left breast/CW target volume. LADCA situated anteriorly in the interventricular groove, received the highest mean dose in both node-positive and node-negative BC patients, followed by the LV (Fig. 2). This shows the direct exposure of these substructures to tangential photon fields. In contrast, RA and LCx, which are located posteriorly, received lower doses.

While proximity generally correlates with higher doses, interpatient variability (as seen in $LADCA \pm 6.4$ Gy) shows that individual anatomical factors such as heart position, breast size, and beam arrangement influence the dose distribution.

Node-positive BC patients received higher mean doses across all substructures compared to node-negative BC patients; however, this difference is not statistically significant ($p = 0.12$), possibly due to limitations in sample size and uneven distribution in the sample sizes between the groups ($n = 39$ vs. $n = 16$). Furthermore, the difference may be attributed to larger treatment volumes encompassing regional nodes, which have led to increased cardiac exposure. Nonetheless, the ranking of substructure doses remained consistent across both node-positive and

node-negative subgroups, underscoring proximity as a primary driver.

The correlation between MHD/MLVD and cardiac substructures varied significantly between node-positive and node-negative subgroups. In node-positive BC patients, MLVD exhibited stronger correlations with anterior cardiac substructures over MHD (e.g., LADCA: $R^2 = 0.67$ vs. MHD $R^2 = 0.63$; RV: $R^2 = 0.90$ vs. MHD $R^2 = 0.69$). Larger treatment volumes (including regional nodes) likely increased cardiac exposure consistency, enhancing MLVD's correlation with the anterior substructures. Similarly, in node-negative BC patients, MLVD exhibited stronger correlations with anterior cardiac substructures over MHD (e.g., LADCA: MLVD $R^2 = 0.53$ vs. MHD $R^2 = 0.52$, RV: MLVD $R^2 = 0.76$ vs. MHD $R^2 = 0.73$) maintaining the same trend as in node-positive BC patients. MLVD outperformed MHD for critical substructures (e.g., LADCA), but it showed diminished correlation for posterior regions (e.g., RA).

The superiority of MLVD over MHD comes from its anatomical proximity to high-dose regions near the treatment field. Unlike MHD, which averages doses across the entire heart, MLVD better captures dose gradients to anterior substructures, aligning with studies that show LV-specific metrics like LV-V5, predict cardiac toxicity more reliably than MHD [31].

Previous studies support the relevance of mean dose in normal tissue complication probability (NTCP) models for specific substructures. Marks et al., [39] demonstrated in their study that the incidence of new perfusion defects increased with larger irradiated LV volumes and higher mean LV doses, showing a significant trend over time. Nilsson et al., [38] discovered that left BC RT with regional nodal irradiation, particularly to the internal mammary chain (IMC), is high-risk and associated with an increased likelihood of coronary artery stenosis in radiation hotspot areas.

However, our findings are contrary to Atkins et al., [26] who showed that mean based metric is insufficient to predict LAD V15 Gy with confidence suggesting that its validity for optimally predicting cardiac events should be reassessed. But, in their study, the mean-based metric assessed was MHD, which MLVD outperformed in the current study. Although no single metric suffices for all substructures, our study shows incremental improvement of MLVD over MHD in estimating doses to high-risk substructures like LADCA.

The linear regression analyses revealed distinct patterns in how MHD and MLVD predict radiation exposure to cardiac substructures, with notable differences between node-positive and node-negative subgroups. In node-positive patients, MLVD showed greater predictive accuracies with anterior and critical substructures. This likely reflects the larger treatment volumes that include

regional nodes, which enhance the consistency of cardiac exposure. Meanwhile, in node-negative patients, the predictive accuracies were weaker than in node-positive patients, likely due to smaller fields and greater anatomical variability. However, MLVD still outperformed MHD for critical and anterior substructures. MLVD's superiority over MHD might be due to its proximity to high-dose regions near the treatment field. This finding aligns with the study Van den Bogaard et al. [31], which shows that LV-specific metrics predict cardiac toxicity more reliably than MHD. While MLVD does not replace substructure-specific delineation, it offers a realistic surrogate for clinics lacking resources for advanced planning.

The study's limitation lies in its retrospective and purely dosimetric focus, lacking assessments of acute and late cardiotoxicity. Future research with a larger sample size evaluating the effects of both acute and late cardiotoxicity should be explored.

Conclusion

Radiation exposure to cardiac substructures during 3D-CRT for left BC was heterogeneous with LADCA receiving the highest mean dose, followed by the LV. MLVD demonstrated superior predictive accuracy over MHD for estimating doses to the LADCA and other substructures, particularly in node-positive patients. However, neither MHD nor MLVD reliably predicted doses to posterior structures underscoring the need for substructure-specific delineation where feasible. While MLVD offers a realistic improvement over MHD in resource-constrained settings, it does not replace the necessity of individualized substructure optimization for precise cardiac-sparing radiotherapy. Future work should incorporate clinical outcomes and advanced imaging techniques, such as cardiac MRI, to enhance NTCP models by utilizing both mean and volume-based parameters.

Abbreviations

| | |
|--------|--|
| 3D-CRT | Three-dimensional conformal radiotherapy |
| BC | Breast cancer |
| CT | Computed tomography |
| DVH | Dose-volume histogram |
| EQD2 | Equivalent dose in 2 grays fraction |
| IMRT | Intensity-modulated radiation therapy |
| LA | Left atrium |
| LCx | Left circumflex |
| LADCA | Left anterior descending coronary artery |
| LV | Left ventricle |
| MHD | Mean heart dose |
| MLVD | Mean left ventricular dose |
| NTCP | Normal tissue complication probability |
| OAR | Organs at risk |
| PTV | Planning tumour volume |
| RA | Right atrium |
| RC | Right coronary |
| RTOG | Radiotherapy and oncology group |
| RV | Right ventricle |
| TV | Target volume |
| TPS | Treatment planning system |
| VMAT | Volumetric-modulated arc therapy |

Acknowledgements

The authors would like to express their gratitude to USM, all the staff at the Radiotherapy and Oncology Unit, Advanced Medical and Dental Institute, USM, for their invaluable assistance throughout the research.

Author contributions

NKAK and GK conceived the study design and analysis. MGN, KS, and MM performed data measurement and analysis and drafted the manuscript. MGN and HMZ coordinated the study and participated in discussions and manuscript preparation. All authors read and approved the final manuscript.

Funding

This research was supported by USM RUI grant (1001.CIPPT.8012337).

Data availability

No datasets were generated or analysed during the current study.

Declarations

Ethics approval and consent to participate

The study was approved by the Research Ethics Committee of Universiti Sains Malaysia (USM/JEPeM/16110523).

Consent for publication

Not applicable.

Competing interests

The authors declare no competing interests.

Author details

¹Department of Biomedical Imaging, Advanced Medical and Dental Institute, Universiti Sains Malaysia, Bertam, Kepala Batas, Pulau Pinang 13200, Malaysia

²Department of Medical Radiography, Faculty of Allied Health Sciences, College of Medical Sciences, University of Maiduguri, Bama Road, Maiduguri 1069, Nigeria

³Breast Cancer Translational Research Programme (BCTRP), Advanced Medical & Dental Institute, Universiti Sains Malaysia, Bertam, Kepala Batas, Pulau Pinang 13200, Malaysia

⁴Heart Failure Research Initiative, Advanced Medical & Dental Institute, Universiti Sains Malaysia, Bertam, Kepala Batas, Pulau Pinang 13200, Malaysia

⁵Department of Radiology, School of Medical Sciences, Universiti Sains Malaysia, Health Campus, Kubang Kerian, Kelantan 16150, Malaysia

⁶Cardiology Department, Hospital Lam Wah Ee, Jalan Tan Sri Teh Ewe Lim, George Town, Pulau Pinang 11600, Malaysia

Received: 9 December 2024 / Accepted: 20 February 2025

Published online: 29 April 2025

References

1. Reicht A. Radiation-induced heart disease after breast cancer treatment: how big a problem, and how much can - And should - We try to reduce it? *J Clin Oncol*. 2017;35:1146–8. <https://doi.org/10.1200/JCO.2016.71.4113>.
2. Garg A, Kumar P. Dosimetric Comparison of the Heart and Left Anterior Descending Artery in Patients With Left Breast Cancer Treated With Three-Dimensional Conformal and Intensity-Modulated Radiotherapy. *Cureus*. 2022. <https://doi.org/10.7759/cureus.21108>
3. Ferini G, Valenti V, Viola A, Umana GE, Martorana E. A critical overview of predictors of heart sparing by Deep-Inspiration-Breath-Hold irradiation in Left-Sided breast Cancer patients. *Cancers (Basel)*. 2022;14. <https://doi.org/10.3390/cancers14143477>.
4. Chakraborty S, Chatterjee S. Adjuvant radiation therapy in breast cancer: recent advances & Indian data. *Indian J Med Res*. 2021;154:189–98. https://doi.org/10.4103/ijmr.IJMR_565_20.
5. Gerardina S, Edy I, Sonia S, Cristina DV, Germana RC, Diego G, et al. A new three-dimensional conformal radiotherapy (3DCRT) technique for large breast and/or high body mass index patients: evaluation of a novel fields assessment aimed to reduce extra-target-tissue irradiation. *Br J Radiol*. 2016;89. <https://doi.org/10.1259/bjr.20160039>.
6. Chang JS, Chang JH, Kim N, Kim YB, Shin KH, Kim K. Intensity modulated radiotherapy and volumetric modulated Arc therapy in the treatment of breast cancer: an updated review. *J Breast Cancer*. 2022;25:349–65. <https://doi.org/10.4048/jbc.2022.25.e37>.
7. Duane F, Aznar MC, Bartlett F, Cutter DJ, Darby SC, Jaggi R, et al. A cardiac contouring atlas for radiotherapy. *Radiother Oncol*. 2017;122:416–22. <https://doi.org/10.1016/j.radonc.2017.01.008>.
8. Zhu Q, Kirova YM, Cao L, Arsene-Henry A, Chen J. Cardiotoxicity associated with radiotherapy in breast cancer: A question-based review with current literatures. *Cancer Treat Rev*. 2018;68:9–15. <https://doi.org/10.1016/j.ctrv.2018.03.008>.
9. Loap P, Fourquet A, Kirova Y. Should we move beyond mean heart dose?? *Int J Radiat Oncol Biol Phys*. 2020;107:386–7. <https://doi.org/10.1016/j.ijrobp.2020.02.017>.
10. Ratosia I, Jenko A, Slijivic Z, Pirnat M, Oblak I. Breast size and dose to cardiac substructures in adjuvant three-dimensional conformal radiotherapy compared to tangential intensity modulated radiotherapy. *Radiol Oncol*. 2020;54:470–9. <https://doi.org/10.2478/raon-2020-0050>.
11. Darby SC, Ewertz M, McGale P, Bennet AM, Blom-Goldman U, Brønnum D, et al. Risk of ischemic heart disease in women after radiotherapy for breast Cancer. *N Engl J Med*. 2013;368:987–98. <https://doi.org/10.1056/nejmoa1209825>.
12. Whelan TJ, Olivetto IA, Parulekar WR, Ackerman I, Chua BH, Nabid A, et al. Regional nodal irradiation in Early-Stage Breast Cancer. *N Engl J Med*. 2015;373:307–16. <https://doi.org/10.1056/nejmoa1415340>.
13. Morris ED. Incorporating Cardiac Substructures Into Radiation Therapy For Incorporating Cardiac Substructures Into Radiation Therapy For Improved Cardiac Sparing Improved Cardiac Sparing. 2020.
14. Jacob S, Camilleri J, Derreumaux S, Walker V, Lairez O, Lapeyre M, et al. Is mean heart dose a relevant surrogate parameter of left ventricle and coronary arteries exposure during breast cancer radiotherapy: A dosimetric evaluation based on individually-determined radiation dose (BACCARAT study). *Radiat Oncol*. 2019;14. <https://doi.org/10.1186/s13014-019-1234-z>.
15. Morris ED, Aldridge K, Ghanem AI, Zhu S, Glide-Hurst CK. Incorporating sensitive cardiac substructure sparing into radiation therapy planning. *J Appl Clin Med Phys*. 2020;21:195–204. <https://doi.org/10.1002/acm2.13037>.
16. Abdullah R, Appalanaido GK, Shukor SA, Zin HM, Aziz MZA, Ishak N. Lateral wedge with medial only cardiac shielding (LEMONADE) technique in left chest wall adjuvant radiotherapy. *Rep Practical Oncol Radiotherapy*. 2021;26:892–8. <https://doi.org/10.5603/RPOR.a2021.0105>.
17. Kunheri B, Kotne S, Nair S, Makuny D. A dosimetric analysis of cardiac dose with or without active breath coordinator moderate deep inspiratory breath hold in left sided breast cancer radiotherapy. *J Cancer Res Ther*. 2017;13:56–61. https://doi.org/10.4103/jcrt.JCRT_1414_16.
18. Mezenski P, Kukolowicz P. What new dose distribution statistics May be included in the optimization of dose distribution in radiotherapy for post-mastectomy patients. *Nowotwory*. 2021;71:267–73. <https://doi.org/10.5603/NJO.a2021.0047>.
19. Naimi Z, Moujahed R, Neji H, Yahyaoui J, Hamdoun A, Bohli M, et al. Cardiac substructures exposure in left-sided breast cancer radiotherapy: is the mean heart dose a reliable predictor of cardiac toxicity? *Cancer/Radiotherapie*. 2021;25:229–36. <https://doi.org/10.1016/j.canrad.2020.09.003>.
20. Piroth MD, Baumann R, Budach W, Dunst J, Feyrer P, Fietkau R, et al. Heart toxicity from breast cancer radiotherapy: current findings, assessment, and prevention. *Strahlenther Onkol*. 2019;195. <https://doi.org/10.1007/s00066-018-1378-z>.
21. Yadav B, Sood A, Dahiya D. 152 (PB-065) Poster - Late cardiac effects in patients with left breast cancer treated with hypofractionated radiotherapy. *Eur J Cancer*. 2022;175:S48. [https://doi.org/10.1016/S0959-8049\(22\)01479-4](https://doi.org/10.1016/S0959-8049(22)01479-4).
22. Hoppe BS, Bates JE, Mendenhall NP, Hoppe RT, Morris CG, Li Z, et al. The relationship of mean heart dose and cardiac substructure dose over evolving radiation techniques in mediastinal lymphoma. *Int J Radiation Oncology*Biophysics*. 2018;102:S87. <https://doi.org/10.1016/j.ijrobp.2018.06.228>.
23. Choi MS, Choi BS, Chung SY, Kim N, Chun J, Kim YB, et al. Clinical evaluation of atlas- and deep learning-based automatic segmentation of multiple organs and clinical target volumes for breast cancer. *Radiother Oncol*. 2020;153:139–45. <https://doi.org/10.1016/j.radonc.2020.09.045>.
24. McWilliam A, Kennedy J, Hodgson C, Vasquez Osorio E, Favier-Finn C, van Herk M. Radiation dose to heart base linked with poorer survival in lung

- cancer patients. *Eur J Cancer*. 2017;85:106–13. <https://doi.org/10.1016/j.jejca.2017.07.053>.
25. Zhang N, Liu X, Tao D, Wang Y, Wu Y, Zeng X. Optimal radiotherapy modality sparing for cardiac valves in left-sided breast cancer. *Ann Transl Med*. 2023;11:46–46. <https://doi.org/10.21037/atm-22-6633>.
 26. Atkins KM, Bitterman DS, Chaunzwa TL, Kozono DE, Baldini EH, Aerts HJWL, et al. Mean heart dose is an inadequate surrogate for left anterior descending coronary artery dose and the risk of major adverse cardiac events in lung Cancer radiation therapy. *Int J Radiat Oncol Biol Phys*. 2021;110:1473–9. <https://doi.org/10.1016/j.ijrobp.2021.03.005>.
 27. Lee J, Hua KL, Hsu SM, Lin J, Bin, Lee CH, Lu KW, et al. Development of delineation for the left anterior descending coronary artery region in left breast cancer radiotherapy: an optimized organ at risk. *Radiother Oncol*. 2017;122:423–30. <https://doi.org/10.1016/j.radonc.2016.12.029>.
 28. Whiteman S, Alimi Y, Carrasco M, Gielecki J, Zurada A, Loukas M. Anatomy of the cardiac chambers: A review of the left ventricle. *Translational Res Anat*. 2021;23. <https://doi.org/10.1016/j.tria.2020.100095>.
 29. Faletra FF, Narula J, Siew , Ho Y. Atlas of Non-Invasive imaging in cardiac anatomy. Gewerbestrasse 11, 6330 Cham. Switzerland: Springer Nature Switzerland AG; 2020.
 30. Averbeck D. Radiosensitivity of the heart. *Open J Cardiol Heart Dis*. 2018. <http://doi.org/10.31031/OJCHD.2018.02.000535>.
 31. n Den Bogaard VAB, Van Der Ta BDP, Bouma AB, Middag AMH, Bantema-Joppe EJ, et al. Validation and modification of a prediction model for acute cardiac events in patients with breast cancer treated with radiotherapy based on three-dimensional dose distributions to cardiac substructures. *J Clin Oncol*. 2017;35:1171–8. <https://doi.org/10.1200/JCO.2016.69.8480>.
 32. Sardaro A, Petruzzelli MF, D'Errico MP, Grimaldi L, Pili G, Portaluri M. Radiation-induced cardiac damage in early left breast cancer patients: risk factors, biological mechanisms, radiobiology, and dosimetric constraints. *Radiother Oncol*. 2012;103:133–42. <https://doi.org/10.1016/j.radonc.2012.02.008>.
 33. JASP Team. JASP (Version 0.18.0)[Computer software] 2023.
 34. Duma MN, Herr AC, Borm KJ, Trott KR, Molls M, Oechsner M, et al. Tangential field radiotherapy for breast cancer—the dose to the heart and heart subvolumes: what structures must be contoured in future clinical trials? *Front Oncol*. 2017;7. <https://doi.org/10.3389/fonc.2017.00130>.
 35. Tong Y, Yin Y, Cheng P, Lu J, Liu T, Chen J, et al. Quantification of variation in dose-volume parameters for the heart, pericardium and left ventricular myocardium during thoracic tumor radiotherapy. *J Radiat Res*. 2018;59:462–8. <https://doi.org/10.1093/jrr/rry026>.
 36. Costin IC, Marcu LG. Evaluation of heart substructures as a function of dose and Radiation-Induced toxicities in Left-Sided breast Cancer radiotherapy. *Eur J Cancer Care (Engl)*. 2024;2024. <https://doi.org/10.1155/2024/1294250>.
 37. Prunaretty J, Bourgier C, Gourgou S, Lemanski C, Azria D, Fenoglio P. Different meaning of the mean heart dose between 3D-CRT and IMRT for breast cancer radiotherapy. *Front Oncol*. 2023;12. <https://doi.org/10.3389/fonc.2022.1066915>.
 38. Nilsson G, Holmberg L, Garmo H, Duvernoy O, Sjögren I, Lagerqvist B, et al. Distribution of coronary artery stenosis after radiation for breast cancer. *J Clin Oncol*. 2012;30:380–6. <https://doi.org/10.1200/JCO.2011.34.5900>.
 39. Marks LB, Yu X, Prosnitz RG, Zhou SM, Hardenbergh PH, Blazing M, et al. The incidence and functional consequences of RT-associated cardiac perfusion defects. *Int J Radiat Oncol Biol Phys*. 2005;63:214–23. <https://doi.org/10.1016/j.ijrobp.2005.01.029>.

Publisher's note

Springer Nature remains neutral with regard to jurisdictional claims in published maps and institutional affiliations.